Electronics **2015**, *4*, 785-798; doi:10.3390/electronics4040785

OPEN ACCESS

electronics

ISSN 2079-9292

www.mdpi.com/journal/electronics

Article

Performance Analysis of Heterodyne-Detected OCDMA Systems Using PolSK Modulation over a Free-Space Optical Turbulence Channel

Fan Bai [1,*], Yuwei Su [2] and Takuro Sato [1]

[1] Graduate School of Global Information and Telecommunication Studies, Waseda University, 66 bldg., 3-14-9 Ookubo, Shinjuku-ku, Tokyo, Japan; E-Mail: t-sato@waseda.jp

[2] Department of Communications and Computer Engineering, Waseda University, 66 bldg., 3-14-9 Ookubo, Shinjuku-ku, Tokyo, Japan; E-Mail: bruce.suyuwei@gmail.com

* Author to whom correspondence should be addressed; E-Mail: baifan@ruri.waseda.jp; Tel.: +81-3-5286-2816.

Academic Editor: Lei Liu

Received: 30 August 2015 / Accepted: 12 October 2015 / Published: 16 October 2015

Abstract: This paper presents a novel model of heterodyne-detected optical code-division multiple-access (OCDMA) systems employing polarization shift keying (PolSK) modulation over a free-space optical (FSO) turbulence channel. In this article, a new transceiver configuration and detailed analytical model for the proposed system are provided and discussed, taking into consideration the potential of heterodyne detection on mitigating the impact of turbulence-induced irradiance fluctuation on the performance of the proposed system under the gamma-gamma turbulence channel. Furthermore, we derived the closed-form expressions for the system error probability and outage probability, respectively. We determine the advantages of the proposed modeling by performing a comparison with a direct detection scheme obtained from an evaluation of link performance under the same environment conditions. The presented work also shows the most significant impact factor that degrades the performance of the proposed system and indicates that the proposed approach offers an optimum link performance compared to conventional cases.

Keywords: polarization modulation; optical CDMA (OCDMA); free-space optical (FSO); heterodyne detection; gamma-gamma turbulence model

---

1. Introduction

Optical wireless communication (OWC), known as free-space optical (FSO) communication, is considered to be a cost-effective, high-capacity communication technology that provides a practical solution to the last mile problem. However, since the propagation links are over the atmospheric channel, the laser beam will experience the effects of turbulence, referred to as irradiance fluctuation, phase aberration and changes in the degree of polarization (DOP) [1], which can impair the performance of FSO communications significantly. Therefore, various kinds of methods, such as diversity techniques [2] and robust modulation schemes, have been proposed to overcome the degradation of the performance of FSO links due to the turbulence effects [3,4]

The intensity modulation with direct detection (IM/DD) scheme has been wildly utilized in FSO communication. Meanwhile, on-off keying (OOK) is often known as a dominant modulation scheme employed in IM/DD FSO communication systems because of the ease of implementation and bandwidth efficiency [1]. However, when an optical beam propagates through the atmosphere, the performance of the system using OOK modulation is highly sensitive to intensity fluctuation [5]. Hence, an adaptive threshold technology is required to achieve an improved performance in the presence of turbulence effects, which thus adds to the complexity of the receiver configuration [6]. Different from the IM-based FSO system, various PolSK modulation schemes have been adopted in [7–9], where information is encoded as different states of polarization (SOP) by using an external modulator. In [10], the experiment results show that the SOP has much more stable properties compared to the amplitude and phase in the actual case of the laser beam propagation. The PolSK-based FSO system offers an improved link performance in terms of the peak optical power, which can be used as an effective method for reducing the influence of turbulence effects, in the literature [8,9].

In order to enhance the capacity of transmission channel by supporting multiple users in a practical access environment, optical code-division multiple-access (OCDMA) systems have been proposed, particularly in optical fiber networks [11], and also have attracted much attention in FSO communications. In [12], the first time experiment demonstrates that the OCDMA signal can be applied for FSO communications. In [13], the performance of radio-over-FSO (RoFSO) systems carrying OCDMA signals has been investigated within MAInoise in the presence of turbulence. The potential for combining OCDMA and the polarization modulation scheme to increase the FSO link performance has been thoroughly discussed in our previous work [14]. Moreover, to cover the shortage of directly-detected FSO systems in overcoming the impact of atmospheric turbulence, the use of heterodyne detection as a countermeasure for the turbulence mitigation has been reported in [15,16]; it has been demonstrated that heterodyne detection can offer a better background noise rejection and increased detector sensitivity compared to direct detection. This leads to a potential for channel fading reduction, especially at the high values of turbulence intensity.

For the reasons given above, such a study to combine the PolSK-based OCDMA technology and heterodyne detection will be important in designing and optimizing the method to enhance the FSO link performance in the operation environment, combining the advantages of high transmission capacity by multiplexing technology and efficient compensation for the turbulence-induced degradation of signal quality. This work aims at demonstrating the potential of the proposed system in combating the degradation of the signal quality in the presence of turbulence, taking into consideration the turbulence-induced fading and interference noise affecting the link performance. Besides, a performance comparison between heterodyne detection and direct detection applied in a OCDMA FSO link has been also analyzed.

The rest of the paper is organized as follows: we introduce a statistical model to describe the irradiance fluctuation across the whole turbulence regimes in Section 2; in Section 3, the mathematical model for describing the PolSK-based OCDMA signal transmission through the FSO turbulence link with heterodyne detection is provided; the results are discussed in Section 4; the conclusions are presented in Section 5.

2. Optical Scintillation Effect

Irradiance fluctuation, known as optical scintillation, has been recognized as an important influence factor on FSO link performance, which is mainly caused by random fluctuations of the refractive index due to temperature, pressure and wind variations along the propagation path of the turbulence channel [17]. The widely-accepted turbulence channel model is the gamma-gamma distribution, which provides a statistical description of irradiance fluctuation in varying degrees of turbulence strength. The probability density function (PDF) of the gamma-gamma turbulence model can be described as [17]:

$$f_X(X)_{G-G} = \frac{2(\alpha\beta)^{\frac{\alpha+\beta}{2}}}{\Gamma(\alpha)\Gamma(\beta)}(X)^{\frac{\alpha+\beta}{2}-1} K_{\alpha-\beta}(2\sqrt{\alpha\beta X}), X > 0 \tag{1}$$

where $X = I/\langle I \rangle$, I is a random variable of the signal current and the symbol $\langle . \rangle$ denotes the average over scintillation. $\Gamma(.)$ is the gamma function, and $K_n(.)$ and λ denote a modified Bessel function of the second kind of order n and operating wavelength, respectively; the parameters α and β represent the small-scale and large-scale irradiance fluctuation and are defined for a spherical wave with aperture averaging (AA) as [17]:

$$\alpha = \left\{ exp\left[\frac{0.49\sigma^2}{\left(1 + 0.18d^2 + 0.56\sigma^{12/5}\right)^{-7/6}} \right] - 1 \right\}^{-1} \tag{2}$$

$$\beta = \left\{ exp\left[\frac{0.51\sigma^2 \left(1 + 0.69\sigma^{12/5}\right)^{-5/6}}{\left(1 + 0.9d^2 + 0.62d^2\sigma^{12/5}\right)} \right] - 1 \right\}^{-1} \tag{3}$$

where $\sigma^2 = 0.5w^{7/6}C_n^2L^{11/6}$ denotes the Rytov variance, $d = \sqrt{wD^2/4L}$, D is the aperture diameter, $w = 2\pi/\lambda$ is the wave number, C_n^2 denotes the turbulence structure index of the refraction constant and L is the transmission distance. The scintillation index S can be derived by α and β as $S = 1/\alpha + 1/\beta + 1/\alpha\beta$. [17]

3. PolSK-OCDMA Systems with Heterodyne Detection over FSO Links

In this section, a mathematical modeling that can be used to characterize the performance of the proposed system was provided. Conventionally, the property of OCDMA technology relies mainly on the characteristics of the signature sequences for users, such as code length and code weight [18]. We take advantage of correlation properties of the modified prime codes (MPCs) with code length p^2 and code weight p to present the system performance in this analysis, where p is a prime code parameter.

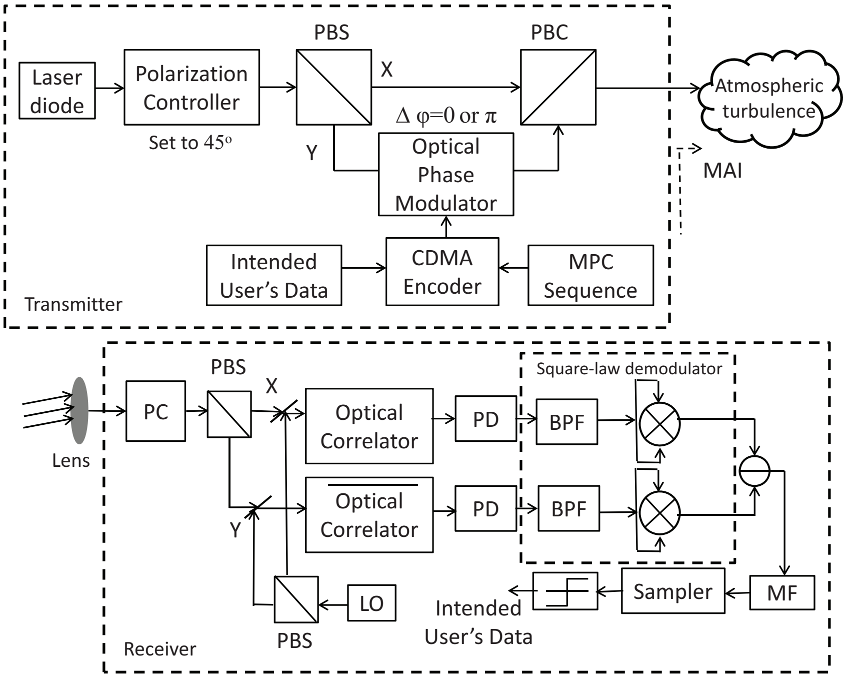

Figure 1. PolSK-optical code-division multiple-access (OCDMA) systems with heterodyne detection over turbulent FSO links. PD, photo-detector; BPF, band-pass filter.

3.1. Modeling of the Transmitter and Receiver

The basic configuration of the proposed systems is illustrated in Figure 1. At the transmitter side, the transmitted laser beam is set to be linearly polarized at an angel of $\pi/4$ as a transmitter reference axis by using a polarization controller (PC) and then is fed into the polarization beam splitter (PBS) and split into two equal beams with $\hat{x}$ and $\hat{y}$ polarization components, respectively, while only the $\hat{y}$-component is phase modulated by using a optical phase modulator between zero and π depending on the input data stream. Therefore, under this assumption, each incoming user's data are encoded by means of an MPC signature sequence and then alternatively mapped into two linear orthogonal states of polarization (SOPs) of the laser beam with a constant envelop. Consequently, the output from a polarization beam combiner (PBC) for the k-th user can be written as:

$$E_{T.k}(t) = \sqrt{\frac{P_{t.k}}{2}} exp\left[j\left(\omega_s t + \varphi_s(t)\right)\right]\left\{\hat{x} + exp\left(j\Delta\varphi\right)\hat{y}\right\} \tag{4}$$

where $P_{t.k}$ denotes the transmitted optical power and ω_s and $\varphi_s(t)$ denote the carrier frequency of the beam and transmitter laser phase noise, respectively. The $\Delta\varphi(t)$=$S_k(t)\cdot\pi$ is the SOP phase information to be transmitted for the k-th user, $S_k(t) = [0, 1]$. Moreover, it should be noted that the k-th user transmitted optical CDMA signal can be defined as $S_k(t) = d_k(t)c_k(t)$, and $d_k(t) = \sum_{i=0}^{M-1} d_{k,i}P_T(t - iT_s)$ and $c_k(t) = \sum_{i=0}^{N-1} d_{k,i}P_T(t - iT_c)$ represent the intended user data with M bits and the signature address with N chips, respectively, with $d_k(t)$, $c_k(t) = [0, 1]$, P_{T_s} being the unity rectangular pulse, where T_s

and T_c denote the symbol duration and chip duration, respectively, $0 \leq t \leq T_s$ and $0 \leq t \leq T_c$; and $T_s/T_c = p^2$.

Moreover, polarized light also can be expressed by the Jones representation in terms of the vector field, and the Jones matrix is described as $J = \left[E_x, E_y\right]^T$. The transmitted signal denoted by the Jones vector thus can be defined as $J^0 = \frac{1}{\sqrt{2}}[1,1]^T$ and $J^1 = \frac{1}{\sqrt{2}}[-1,1]^T$ for the data bits "0" and "1", respectively, where J^0 and J^1 are orthogonal to each other [18]. Hence, we have a unit complex Jones matrix represented by $Q = \left[J^0, J^1\right]$. With this, the optical signal is then transmitted through the turbulence link.

The optical signal suffers from the combined effects of the channel fading and interference noise while propagating through the atmosphere. The received signal that propagates from the channel can be expressed as $\sum_{k=1}^{K} S_k(t-\tau_k)$, where τ_k, $0 \leq \tau_k \leq T_s$ is the time delay between the desired user and k-th user. Thus, the overall field vectors in the channel is given:

$$E_{channel}(t) = \sum_{k=1}^{K} E_{T.k}(t) \cdot h + E_{FSO}(t) \tag{5}$$

where h models the channel fading of the propagation path, and this modeling is defined as $h = L_a L_p X(t)$; L_a is the atmospheric attenuation, including the rain and visibility losses, L_r and L_v, respectively; $L_r = aLR^b$ (dB) with R being the rainfall rate (mm/h); a and b are given according to the location; $L_v = \left\{\left[13L\left(\left(\lambda \times 10^9\right)/\left(500\right)\right)^{-\sigma(V)}\right]/V\right\}$ (dB) with V (km) being the visibility; and $\sigma(V)$ is the particle size distribution coefficient, defined with the Kim model as [13]:

$$\sigma(V) \begin{cases} 1.6 & V > 50km \\ 1.3 & 6km < V < 50km \\ 0.16V + 0.34 & 1km < V < 6km \\ V - 0.5 & 0.5km < V < 1km \\ 0 & V < 0.5km \end{cases} \tag{6}$$

L_p is geometric spread and pointing error losses, and $X(t)$ the quantifies variation of the channel fading in terms of optical scintillation due to the turbulence effects and is satisfied with the gamma-gamma turbulence model, as mentioned earlier. $E_{FSO}(t)$ denotes the field vector of additive Gaussian white noise (AWGN).

In the analysis to follow, the mathematical modeling for PolSK-OCDMA signal processing based on heterodyne detection is presented. The received composite signal outputs from the $1 \times K$ optical splitter (OS) for a single receiver are expressed as follows [19,20]:

$$\begin{aligned} E_R(t,X) = Re\Bigg\{ & E_0(t) exp\left[j(\omega_s t + \varphi_r(t))\right] \\ & \times \sum_{k=1}^{K} Q \begin{bmatrix} d_k(t) \\ 1 - d_k(t) \end{bmatrix} c_k(t) P_T(t - kT_S) \Bigg\} \end{aligned} \tag{7}$$

In the formula, $Re\{.\}$ represents the real part of $E_R(t,X)$; the electromagnetic filed vector of the k-th user before the external modulation is defined as $E_0(t) = [E_x(t), E_y(t)]^T$. The $\varphi_r(t) = \varphi_s(t) + \varphi_c(t)$ is the overall phase noise from the transmitter to the input of the receiver with the $\varphi_c(t)$ representing the phase noise induced from a turbulent channel. The turbulence-induced SOP fluctuation is compensated by using the polarization controller (PC), whose function is to ensure that the received optical beam has the same SOP reference axis as the transmitter side. Thus, both of the received orthogonal components are assumed as being equally amplitude and turbulence fluctuated without the loss of orthogonality between the two orthogonal polarizations.

The power of the local oscillator laser source is equally split by the PBS between the x and y component, linearly polarized at $\pi/4$, and thus, the local oscillator (LO) signal $E_{LO}(t)$ of the desired user (e.g., the first user) is given by:

$$E_{LO}(t) = \sqrt{\frac{P_{LO}}{2}} exp\left[j(\omega_{LO}t + \varphi_{LO}(t))\right]\{\hat{x} + \hat{y}\} \tag{8}$$

The parameters P_{LO}, ω_{LO} and $\varphi_{LO}(t)$ denote the power, angular frequency and local oscillator phase noise generated from the heterodyne receiver, respectively. The received composite signals in both the upper branch (x-component) and lower branch (y-component) are then coherently combined with the local optical field of $E_{LO}(t)$ in using the 3-dB balanced directional coupler within a balanced intensity coupling ratio; thus, the mixed electric field consequently can be written as:

$$E_{upper}(t, X) = \{E_{R.x}(t, X) + E_{LO.x}(t)\}\, \hat{x} \tag{9}$$

$$E_{lower}(t, X) = \{E_{R.y}(t, X) + E_{LO.y}(t)\}\, \hat{y} \tag{10}$$

Moreover, the x-component in the upper branch is given by [19,20]:

$$E_{R.x}(t, X) = \left(\frac{E_{x.k} + E_{y.k}}{2} + \sum_{k=1}^{K} d_k(t)c_k(t)\frac{E_{x.k} - E_{y.k}}{2} P_T(t - kT_S)\right) \tag{11}$$

and the y-component in the lower branch is defined similarly as [19,20]:

$$E_{R.y}(t, X) = \left(\frac{E_{x.k} - E_{y.k}}{2} + \sum_{k=1}^{K} d_k(t)c_k(t)\frac{E_{x.k} + E_{y.k}}{2} P_T(t - kT_S)\right) \tag{12}$$

where $E_{x.k} = J^0 d_k(t)c_k(t)E_0(t)$ and $E_{y.k} = J^1(1 - d_k(t))c_k(t)E_0(t)$ are orthogonal components of the k-th user. This regards the processing of the OCDMA signal decoding; the optical correlator known as a simple decoder structure was adopted in the proposed system configuration, which correlates the incoming signals by preserving the desired user's signature sequence to de-spread the encoded signals [21]. Hence, a complement of the code is set to the lower branch.

The optical fields are detected by the dual detectors with unit area to generate differential current ready for extraction in the following processing. The outputs of identical dual detectors are passed through electric bandpass filters (BPFs) with a one-sideband bandwidth B_0. We assume that the BPF bandwidth is larger than the IFlinewidth to avoid the phase noise to amplitude noise conversion [15], and FSO noise, such as background light interference, can be considered negligible in this analysis. The photocurrent after removing the direct-current (DC) and high frequency components in the upper branch can be represented as:

$$\begin{aligned} I^0_{R.x}(t, X) = & \Re X \sum_{n=1}^{N} \left\{ \frac{c(nT_c) + 1}{2} \left[\sum_{k=1}^{K} \sqrt{2P_{LO}} \left(\frac{E_{x.k} + E_{y.k}}{2} \right.\right.\right. \\ & \left.\left.\left. + \; d_k(t)c_k(t - nT_c)\frac{E_{x.k} - E_{y.k}}{2} \right) cos(\omega_{IF}t + \varphi_{IF}(t)) \right] \right\} + n_x(t) \end{aligned} \tag{13}$$

and similarly, the lower branch is given by:

$$\begin{aligned} I^1_{R.y}(t,X) =& \Re X \sum_{n=1}^{N} \left\{ \frac{1-c(nT_c)}{2} \left[\sum_{k=1}^{K} \sqrt{2P_{LO}} \left(\frac{E_{x.k}-E_{y.k}}{2} \right.\right.\right. \\ &+ \left.\left.\left. d_k(t)c_k(t-nT_c)\frac{E_{x.k}+E_{y.k}}{2} \right) cos(\omega_{IF}t+\varphi_{IF}(t)) \right] \right\} + n_y(t) \end{aligned} \tag{14}$$

where $\Re$ denotes the responsivity of the detector, and $\omega_{IF} = \omega_s - \omega_{LO}$ and $\varphi_{IF}(t) = \varphi_r(t) - \varphi_{LO}(t)$ are the frequency and phase noise of the intermediate signal, respectively. In Equations (13) and (14), $n_x(t)$ and $n_y(t)$ indicate the optical link noise and are assumed to be statistically-independent and stationary Gaussian processes with zero-mean and variance of σ^2_{opt}.

Then, the photocurrents $I^0_{R.x}$ and $I^1_{R.y}$ are processed followed by the square-law demodulator. An ideal square-law demodulator can be used to eliminate the intermediate phase noise and recover the information signal [15,16,22]. Then, the total currents of both branches are fed into a subtractor followed by using a matched filter (MF), and differential output between the upper and lower branch over a symbol duration T_s is derived from:

$$C_d(t,X) = \int_{t=0}^{T_s} \left(I^0_{R.X}(t,X)\right)^2 - \left(I^1_{R.y}(t,X)\right)^2 dt \tag{15}$$

Hence, we should note that, when the decision signal is sampled at the $t = T_s$ to obtain the variable decision C_d, the decision rule of the final bit d is defined as:

$$d = \begin{cases} 0 & if \quad C_d < 0 \\ 1 & if \quad C_d \geq 0 \end{cases} \tag{16}$$

3.2. System Error Probability Analysis

Here, we derived the expressions for determining the degree to which heterodyne-detected FSO link-carrying PolSK-based OCDMA signals may be expected to be degraded due to the irradiance fluctuation and interference noise, by calculating the proposed system error probability. For the proposed system modeling in this analysis, we assume that the time delay $\tau_k = 0$ as a synchronized case. Further, based on Equations (13)–(15), the electric signal of MF output over a certain T_s can be modified as follows:

$$C_d(t,X) \propto \frac{(\Re X)^2 P_{LO}}{2} \sum_{n=1}^{N} c(nT_c) \sum_{k=1}^{K} \left(d_k(t)c_k(t-nT_c)(E^2_{x.k}-E^2_{y.k})\right) + n_{opt}(t) \tag{17}$$

Moreover, when we considering the components of the received signal, Equation (16) becomes as:

$$\begin{aligned} C_d(t,X) \propto& \underbrace{\frac{(\Re X)^2 P_{LO}}{2} \sum_{n=1}^{N} c(nT_c)d_1(t)c_1(t-nT_c)(E^2_{x.k}-E^2_{y.k})}_{\text{desired user data}} \\ &+ \underbrace{\frac{(\Re X)^2 P_{LO}}{2} \sum_{n=1}^{N}\sum_{k=2}^{K} c(nT_c)d_k(t)c_k(t-nT_c)(E^2_{x.k}-E^2_{y.k}) + n_{opt}(t)}_{\text{MAI}} \end{aligned} \tag{18}$$

where the first term represents the desired user data and the second term denotes the interference caused by multiple OCDMA users. In the formula, the optical link noise $n_{opt}(t)$ is related to $n_x(t)$ and $n_y(t)$, which are defined as a zero-mean AWGN process, including the shot noise and thermal noise [13], and can be described by:

$$\begin{aligned} \sigma_{opt}^2 &= \sigma_{shot}^2 + \sigma_{th}^2 \\ &= 2q\Re(P_{LO} + P_R)B_0 + \frac{4K_B T_{abs} F_e B_0}{R_L} \end{aligned} \tag{19}$$

where q and K_B are the electron charge and Boltzmann's constant, respectively, T_{abs} denotes the absolute temperature and F_e and R_L represent the noise factor and load resistance, respectively. The detailed parameters of the value are shown in Table 1. As with previous studies on the operation principle of coherent detection technology [23], the power of LO is assumed to be sufficiently high compared to the received signal power, $P_{LO} \gg P_R$, where P_R is characterized by the received optical power. The shot noise can then be calculated as $\sigma_{shot}^2 \approx 2q\Re P_{LO} B_0$ in later calculation. Then, the signal-to-noise ratio (SNR) based on Equations (18) and (19) is derived as:

$$\begin{aligned} SNR(K,X) &= \frac{P_d(t,X)}{\sigma_{MAI}^2 + \sigma_{opt}^2} \\ &= \frac{\frac{(\Re X)^2}{2} P_{LO} \sum_{n=1}^{N} c(nT_c) d_1(t) c_1(t - nT_c)(E_{x.1}^2 - E_{y.1}^2)}{\frac{(\Re X)^2}{2} P_{LO} \sum_{n=1}^{N} \sum_{k=2}^{K} c(nT_c) d_k(t) c_k(t - nT_c)(E_{x.k}^2 - E_{y.k}^2) + \sigma_{opt}^2} \end{aligned} \tag{20}$$

where $P_d(t, X)$ is the expected desired signal power in the presence of turbulence and σ_{MAI}^2 represents the variance of MAI noise arising from the cross-correlation.

Table 1. Numerical parameters. LO, local oscillator.

Parameters	Value
Transmission distance L	1 km
Wavelength λ	1550 nm
Aperture diameter D	150 mm
bandwidth B_0	2 GHz
Absolute temperature T_{abs}	300 k
Detector responsivity $\Re$	0.9 A/W
Electron charge q	1.602×10^{19} C
Noise figure F_e	2 dB
LO optical power P_{LO}	0 dBm
Pointing error loss L_p	1 dB
Visibility loss L_v	0.4 dB [26]

In this analysis, the MPC as the signature sequence has been adopted for the features of auto-correlation and cross-correlation in order to optimize the differential between the desired arrived signal and multiple interferences. The auto-correlation $\sum_{n=1}^{N} c(nT_c)c_1(t - nT_c) = p$ and cross-correlation functions $\sum_{n=1}^{N} c(nT_c)c_k(t - nT_c) = \lambda_c$ are represented in this calculation. According to the theoretical basis for the MPC, the cross-correlation value is the only one that can generate the interference while the codes are from different groups. It is noted that cross-correlation values are satisfied with a uniform distribution among interfering users and letting $P(\lambda_c) = k/p^2 - p$ as the PDF of the variable λ_c [18,19]. Thus, Equation (20) becomes:

$$SNR(K,X) = \frac{1}{\left(\frac{K(K-1)}{p(p^2-p)}\right)^2 + \frac{2\sigma_{opt}^2}{(\Re X)^2 \cdot P_{LO} \cdot d_1(t) \cdot (E_{x.1}^2 - E_{y.1}^2)}} \tag{21}$$

Then, the average bit error probability for binary PolSK-OCDMA systems over the gamma-gamma distribution is given by:

$$\langle P_e \rangle = \int_0^\infty P_e f_X(X)_{G-G} dX \tag{22}$$

We define the bit error probability for the proposed system under the turbulence effect as $P_e = \frac{1}{2} exp(\frac{-SNR(K,X)}{2})$ [24]. To further simplify Equation (22) for the closed-form, we use the expressions $exp(-Z) = G_{0,1}^{1,0}\left[Z|_0^-\right]$ [25] and $K_n(Z) = (1/2)G_{0,2}^{2,0}\left[Z^2/4|_{\frac{n}{2},\frac{-n}{2}}^{--}\right]$ [25], where $G_{c,d}^{a,b}(.)$ is a Meijer-G function. We assume that $SNR(K,X)$ can be approximated by averaging over scintillation, $SNR(K,X) \approx \langle SNR(K,X) \rangle X^2$ [4,13]. Thus, Equation (22) becomes:

$$\langle P_e \rangle = \frac{2^{(\alpha+\beta)}}{8\pi\Gamma(\alpha)\Gamma(\beta)} G_{4,1}^{1,4}\left(\frac{8\langle SNR(K,X)\rangle}{(\alpha\beta)^2}\Big|_{\quad 0}^{\frac{1-\alpha}{2},\ \frac{2-\alpha}{2},\ \frac{1-\beta}{2},\ \frac{2-\beta}{2}}\right) \tag{23}$$

3.3. System Outage Probability Analysis

Evaluation of the reliability of the proposed system over the fading channel can be proven from the calculation of the outage probability. It is defined as the probability that the SNR falls below a target SNR value; then formula is given as $P_{out}(SNR_{th}) = P_r(SNR(K,X) < SNR_{th})$, where SNR_{th} is the threshold SNR value. Let a constant C_{th} be a ratio $C_{th} = \sqrt{SNR_{th}/\langle SNR(K,X)\rangle}$; thus, the outage probability by using a closed-form solution is obtained as [25]:

$$\begin{aligned} P_{out}(SNR_{th}) &= \int_0^{C_{th}} \frac{2(\alpha\beta)^{\frac{\alpha+\beta}{2}}}{\Gamma(\alpha)\Gamma(\beta)} X^{\frac{\alpha+\beta}{2}-1} K_{\alpha-\beta}(2\sqrt{\alpha\beta X}) dX \\ &= \frac{(\alpha\beta)^{\frac{\alpha+\beta}{2}}}{\Gamma(\alpha)\Gamma(\beta)} C_{th} G_{1,3}^{2,1}\left(\alpha\beta C_{th}\Big|_{\frac{\alpha-\beta}{2},\ \frac{\beta-\alpha}{2},\ \frac{\alpha+\beta}{2}}^{1-\frac{\alpha-\beta}{2}}\right) \end{aligned} \tag{24}$$

4. Simulation and Numerical Analysis

In this section, we use simulation and numerical analysis to verify the overall performance of the PolSK-modulated OCDMA systems with heterodyne detection over a FSO turbulence link, taking into account the error probability and outage probability. This analysis uses weak and strong turbulence intensity levels at different Rytov variance values $\sigma = 0.2$ and $\sigma = 5$. The scintillation parameters are $\{\alpha = 11.6, \beta = 10.1\}$, $\{\alpha = 2.6, \beta = 1.3\}$, respectively [27].

As the performance of OOK-based OCDMA FSO system with and without heterodyne detection has been well studied in several literature, we first prefer to give a comparison between OOK with a fixed threshold detection and PolSK modulation under the same link conditions. Figure 2 shows the numerical results of the relationship between the SNR and average BER when the single OCDMA user has no MAI noise and the modified prime code parameter $p = 13$. It is seen that the system average error probability increases as the turbulence strength increases, with system performance under strong turbulence showing the worst case scenario. For instance, when $SNR = 16$ dB for the proposed system, the average BER performance is 1×10^{-7}, 2×10^{-2} under weak and strong turbulence regimes, respectively. This result proves that the quality of the signal is highly sensitive to the turbulence effect. At the same time, it is recognized that the proposed system offers the optimum performance compared to that of the conventional cases. In addition, the system error probability using the heterodyne detection receiver is significantly improved compared to the direct detection mode, especially considered in the case of turbulence conditions. The average BER of both modulation schemes with heterodyne detection can be lower by one order of magnitude than the case of the direct detection in the strong turbulence for the same SNR. Furthermore, using the PolSK modulation scheme also displays a better system performance than OOK with a fixed threshold detection. This result can be explained as it was previously studied that polarization states can maintain much more stable properties when propagating through the turbulence channel. The above-mentioned results indicate that combining the PolSK modulation and coherent detection can be used as an efficient method of turbulence mitigation to overcome the link performance degradation.

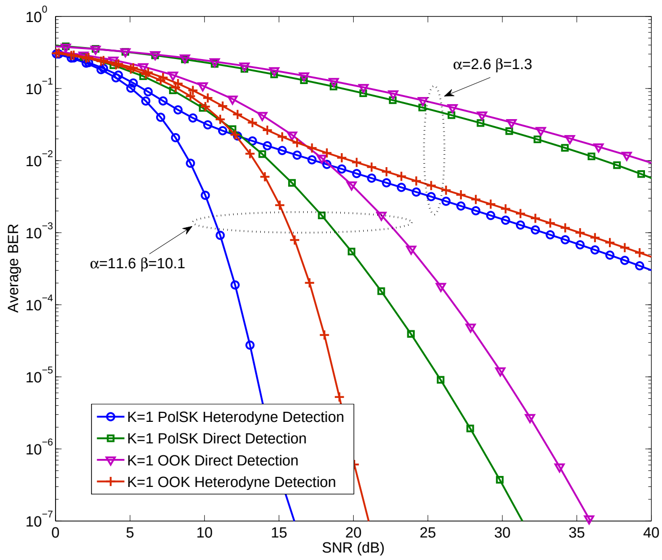

Figure 2. Average BER *versus* electrical SNR when $K = 1$, compared to the system using on-off keying (OOK) under weak and strong turbulence regimes.

Next, we present the results that aim at highlighting the limit of MAI noise to the system loadability under turbulence effects. The average BER performance *versus* the variation of number of active users with MPC parameters, $p = 5$, $p = 13$ and $p = 17$, respectively, in the different turbulence regimes is shown in Figure 3a. For the received optical power $P_R = -20$ dBm, the average BER is decreased when the number of active users increases with respect to the strong interference caused by multiple users. In fact, the conventional CDMA system is able to maintain a credible quality of communication when multiple users share the same link, which mainly depends on the code parameter corresponding to the code-set cardinality p^2 [19]. The average bit error probability improved by the larger of the MPC parameters p, which is related to the higher auto-correlation peaks or lower hit probabilities, as discussed in [20].

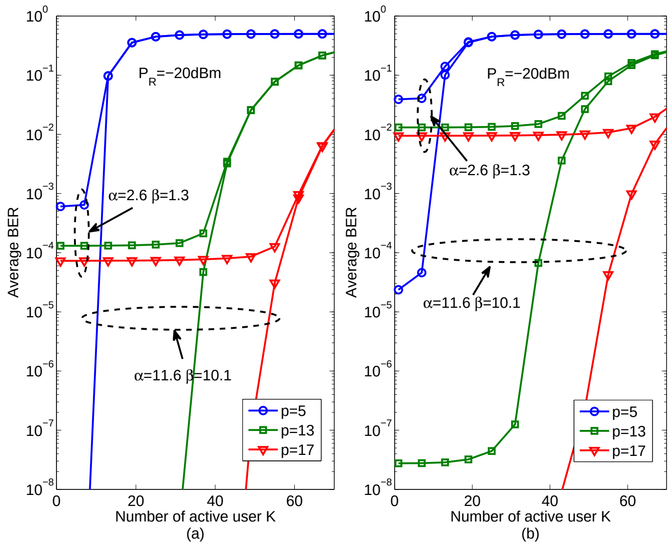

Figure 3. Average BER *versus* the number of active users with different prime code parameters when $P_R = -20$ dBm under the turbulence effect. (**a**) Heterodyne detection; (**b**) direct detection.

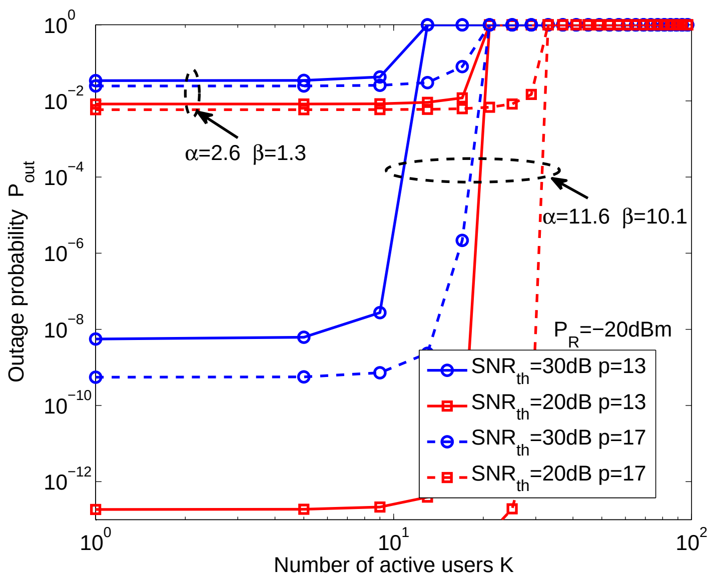

Figure 4. Variation of the outage probability P_{out} *versus* the number of active users K, when $P_R = -20$ dBm under a range of turbulence characteristics.

To continue the performance comparison, both the heterodyne detection and direct detection are under the same link conditions, as shown in Figure 3a,b. It is noted that the performance of heterodyne detection outperforms that of direct detection under the same link conditions, especially in the strong turbulence regimes, where the heterodyne detection can be lower by nearly two orders of magnitude than the case of direct detection in terms of the average BER for the same number of active users.

Therefore, based on the results illustrated in this plot, we can determine that coherent detection is an attractive alternative to-the direct detection, which offers an efficient way to compensate the turbulence induced channel fading.

Finally, it can be observed that outage probability increases as the number of active users increases, as shown in the Figure 4, this is explained as above as being due to the increase of the MAI noise. Two cases of SNR_{th} and prime code parameter p have been considered, $SNR_{th} = (20\text{ dB}, 30\text{ dB})$, $p = (13, 17)$, respectively. For instance, for $SNR_{th} = 20$ dB and $P_{out} = 1 \times 10^{-2}$ with $p = 13$, the number of active users decreases from value $K = 20$ to $K = 12$ across the weak and strong turbulence regimes.

5. Conclusions

This paper combines the advantages of PolSK modulation and heterodyne detection and proposes an analytical model to characterize the performance of PolSK-based OCDMA systems with heterodyne detection over a turbulent FSO link. We derived the closed-form expressions of the system error probability and outage probability over the gamma-gamma turbulence channel. The MPC parameter as a performance metric has been also considered and quantifies the impact of interference noise on the system loadability. The conclusions obtained through numerical simulation indicate that the performance of the propose system is highly sensitive to turbulence-induced irradiance fluctuation and the MAI effect; the choice of heterodyne detection receiver offers an improved FSO link performance compared to the conventional cases and provides an effective and promising method for turbulence mitigation in the field of FSO communications.

Author Contributions

Fan Bai contributed to the original idea. Yuwei Su contributed to the simulation. Takuro Sato is the supervisor of the work.

Conflicts of Interest

The authors declare no conflict of interest.

References

1. Zhu, X.; Kahn, J. Free-space optical communication through atmospheric turbulence channels. *IEEE Trans. Commun.* **2002**, *50*, 1293–1300.
2. Wang, Z.; Zhong, W.; Fu, S.; Lin, C. Performance comparison of different modulation formats over free-space optical (FSO) turbulence links with space diversity reception technique. *IEEE Photonics J.* **2009**, *1*, 277–285.
3. Li, J.; Liu, J.Q.; Taylor, D. Optical Communication Using Subcarrier PSK Intensity Modulation Through Atmospheric Turbulence Channels. *IEEE Trans. Commun.* **2007**, *55*, 1598–1606.
4. Bekkali, A.; Ben Naila, C.; Kazaura, K.; Wakamori, K.; Matsumoto, M. Transmission Analysis of OFDM-Based Wireless Services Over Turbulent Radio-on-FSO Links Modeled by Gamma-Gamma Distribution. *IEEE Photonics J.* **2010**, *2*, 510–520.

5. Gappmair, W.; Hranilovic, S.; Leitgeb, E. OOK Performance for Terrestrial FSO Links in Turbulent Atmosphere with Pointing Errors Modeled by Hoyt Distributions. *IEEE Commun. Lett.* **2011**, *15*, 875–877.
6. Ghassemlooy, Z.; Tang, X.; Rajbhandari, S. Experimental investigation of polarisation modulated free space optical communication with direct detection in a turbulence channel. *Commun. IET* **2012**, *6*, 1489–1494.
7. Zhao, X.; Yao, Y.; Sun, Y.; Liu, C. Circle Polarization Shift Keying With Direct Detection for Free-Space Optical Communication. *J. Opt. Commun. Netw.* **2009**, *1*, 307–312.
8. Zhao, X.; Yao, Y.; Sun, Y.; Xu, X.; Tian, J.; Liu, C. Condition of Keeping Polarization Property Unchanged in the Circle Polarization Shift Keying System. *J. Opt. Commun. Netw. IEEE/OSA* **2010**, *2*, 570–575.
9. Zhao, L.; Lei, Z.-y.; Ren, A.-h.; Ke, X.-z.; Wu, Y.-h. Research on Light Polarization FSO-OFDM System. In Proceedings of 2010 International Conference on Electrical and Control Engineering (ICECE), Wuhan, China, 25–27 June 2010; pp. 4552–4555.
10. Strohbehn, J.; Clifford, S. Polarization and angle-of-arrival fluctuations for a plane wave propagated through a turbulent medium. *IEEE Trans. Antennas Propag.* **1967**, *15*, 416–421.
11. Wang, X.; Kitayama, K. Analysis of beat noise in coherent and incoherent time-spreading OCDMA. *J. Lightw. Technol.* **2004**, *22*, 2226–2235.
12. Sasaki, K.; Minato, N.; Ushikubo, T.; Arimoto, Y. First OCDMA Experimental Demonstration over Free Space and Optical Fiber Link. In Proceedings of the Conference on Optical Fiber communication/National Fiber Optic Engineers Conference, OFC/NFOEC, San Diego, CA, USA, 24–28 February 2008; pp. 1–3.
13. Ben Naila, C.; Bekkali, A.; Wakamori, K.; Matsumoto, M. Performance Analysis of CDMA-Based Wireless Services Transmission Over a Turbulent RF-on-FSO Channel. *J. Opt. Commun. Netw. IEEE/OSA* **2011**, *3*, 475–486.
14. Bai, F.; Su, Y.; Sato, T. Performance Analysis of Polarization Modulated DirectDetection Optical CDMA Systems over Turbulent FSO LinksModeled by the Gamma-Gamma Distribution. *Photonics* **2015**, *2*, 139.
15. Tang, X.; Ghassemlooy, Z.; Rajbhandari, S.; Popoola, W.; Lee, C. Differential Circular Polarization Shift Keying with Heterodyne Detection for Free Space Optical Links with Turbulence Channel. In Proceedings of the 2011 16th European Conference on Networks and Optical Communications (NOC), Newcastle-Upon-Tyne, UK, 20–22 July 2011; pp. 149–152.
16. Tang, X.; Ghassemlooy, Z.; Rajbhandari, S.; Popoola, W.; Lee, C.G. Coherent Heterodyne Multilevel Polarization Shift Keying With Spatial Diversity in a Free-Space Optical Turbulence Channel. *J. Lightw. Technol.* **2012**, *30*, 2689–2695.
17. Andrews, L.C.; Phillips, R.L. *Laser Beam Propagation through Random Media*, 2nd ed.; SPIE: Washington, DC, USA, 2005.
18. Iversen, K.; Junghanns, D. On the Combination of Optical CDMA and POLSK. *J. Opt. Commun.* **1995**, *16*, 126–130.
19. Karbassian, M.; Ghafouri-Shiraz, H. Transceiver Architecture for Incoherent Optical CDMA Networks Based on Polarization Modulation. *J. Lightw. Technol.* **2008**, *26*, 3820–3828.

20. Salehi, J. Code division multiple-access techniques in optical fiber networks. I. Fundamental principles. *IEEE Trans. Commun.* **1989**, *37*, 824–833.
21. Salehi, J.; Brackett, C. Code division multiple-access techniques in optical fiber networks. II. Systems performance analysis. *IEEE Trans. Commun.* **1989**, *37*, 834–842.
22. Cvijetic, N.; Qian, D.; Yu, J.; Huang, Y.K.; Wang, T. Polarization-Multiplexed Optical Wireless Transmission With Coherent Detection. *J. Lightw. Technol.* **2010**, *28*, 1218–1227.
23. Niu, M.; Song, X.; Cheng, J.; Holzman, J.F. Performance analysis of coherent wireless optical communications with atmospheric turbulence. *Opt. Express* **2012**, *20*, 6515–6520.
24. Tang, X.; Ghassemlooy, Z.; Rajbhandari, S.; Popoola, W.; Lee, C.; Leitgeb, E.; Ahmadi, V. Free-space optical communication employing polarization shift keying coherent modulation in atmospheric turbulence channel. In Proceedings of the 2010 7th International Symposium on Communication Systems Networks and Digital Signal Processing (CSNDSP), Newcastle upon Tyne, UK, 21–23 July 2010; pp. 615–620.
25. Adamchik, V.S.; Marichev, O. The algorithm for calculating integrals of hypergeometric type functions and its realization in REDUCE system. In Proceedings of the International Conference Symbolic Algebraic, Tokyo, Japan, 20–24 August 1990; pp. 212–224.
26. Kim, I.I.; McArthur, B.; Korevaar, E.J. Comparison of laser beam propagation at 785 nm and 1550 nm in fog and haze for optical wireless communications. *Proc. SPIE* **2001**, *4214*, 26–37.
27. Wang, N.; Cheng, J. Moment-based estimation for the shape parameters of the Gamma-Gamma atmospheric turbulence model. *Opt. Express* **2010**, *18*, 12824–12831.